A vessel noise budget for Admiralty Inlet, Puget Sound, Washington (USA)

Christopher Bassett[a] and Brian Polagye
Department of Mechanical Engineering, University of Washington, Seattle, Stevens Way, Box 352600, Seattle, Washington 98165

Marla Holt
Conservation Biology Division, Northwest Fisheries Science Center, National Marine Fisheries Service, National Oceanic and Atmospheric Administration, 2725 Montlake Boulevard East, Seattle, Washington 98112

Jim Thomson
Applied Physics Laboratory, University of Washington, Seattle, 1013 Northeast 40th Street, Box 355640, Seattle, Washington 98105-6698

(Received 18 March 2012; revised 3 August 2012; accepted 28 September 2012)

One calendar year of Automatic Identification System (AIS) ship-traffic data was paired with hydrophone recordings to assess ambient noise in northern Admiralty Inlet, Puget Sound, WA (USA) and to quantify the contribution of vessel traffic. The study region included inland waters of the Salish Sea within a 20 km radius of the hydrophone deployment site. Spectra and hourly, daily, and monthly ambient noise statistics for unweighted broadband (0.02–30 kHz) and marine mammal, or M-weighted, sound pressure levels showed variability driven largely by vessel traffic. Over the calendar year, 1363 unique AIS transmitting vessels were recorded, with at least one AIS transmitting vessel present in the study area 90% of the time. A vessel noise budget was calculated for all vessels equipped with AIS transponders. Cargo ships were the largest contributor to the vessel noise budget, followed by tugs and passenger vessels. A simple model to predict received levels at the site based on an incoherent summation of noise from different vessels resulted in a cumulative probability density function of broadband sound pressure levels that shows good agreement with 85% of the temporal data. © *2012 Acoustical Society of America*. [http://dx.doi.org/10.1121/1.4763548]

PACS number(s): 43.30.Nb, 43.50.Lj, 43.50.Cb, 43.50.Rq [AMT] Pages: 3706–3719

I. INTRODUCTION

The impacts of high energy, impulsive sources of anthropogenic sounds such as sonars and seismic exploration on marine species have been an area of active research (NRC, 2000, 2003). Increasingly, concerns have expanded to include continuous, lower energy sources such as shipping traffic. Low-frequency ambient noise levels in the open ocean have long been attributed to maritime traffic (Wenz, 1962; Urick, 1967; Ross, 1976; Greene and Moore, 1995; McDonald *et al.*, 2006; McDonald *et al.*, 2008; Hildebrand, 2009; Frisk, 2012). Low-frequency (<500 Hz), high energy (>180 dB re 1 μPa at 1 m) noise generated by large shipping vessels propagates efficiently across ocean basins, contributing to ambient noise levels over large distances (>100 km). At shorter distances (<10 km), higher frequency noise may also be significant (NRC, 2003).

The acoustic signature (i.e., spectral characteristics) of a vessel depends on its design characteristics (e.g., gross tonnage, draft), on-board equipment (e.g., generators, engines, active acoustics equipment), and operating conditions (e.g., speed, sea state) (Ross, 1976). The primary sound generation mechanism for commercial vessels is cavitation, which produces broadband noise and tonal components related to the rotation rate of the ship propeller (Gray and Greeley, 1980). Source levels for vessels, referenced to dB re 1 μPa at 1 m, range from 150 dB for small fishing vessels and recreational watercraft to 195 dB for super tankers (Gray and Greeley, 1980; Kipple and Gabriele, 2003; Hildebrand, 2005). Peaks in spectral levels for shipping traffic occur at frequencies less than 500 Hz with substantial tonal contributions as low as 10 Hz (Ross, 1976; Scrimger and Heitmeyer, 1991; Greene and Moore, 1995). Small ships are quieter at low frequencies but can approach or exceed noise levels of larger ships at higher frequencies (Greene and Moore, 1995; Kipple and Gabriele, 2003; Hildebrand, 2005). Radiated noise levels are also directional and vary based on vessel orientation or aspect (Arveson and Vendittis, 2000; Trevorrow *et al.*, 2008). In addition to mechanical noise, active acoustics devices are a significant high-frequency noise source due to the widespread use of fish finding and depth sounding devices (NRC, 2005). Source levels for common active acoustics devices are on the order of 150–200 dB at frequencies from 3 to 200 kHz, with the most common commercial devices operating above 50 kHz (NRC, 2003; Hildebrand, 2004). However, downward directionality and rapid attenuation at high frequencies limit their contribution to broadband noise levels over large spatial scales.

[a]Author to whom correspondence should be addressed. Electronic mail: cbassett@uw.edu

 0001-4966/2012/132(6)/3706/14/$30.00

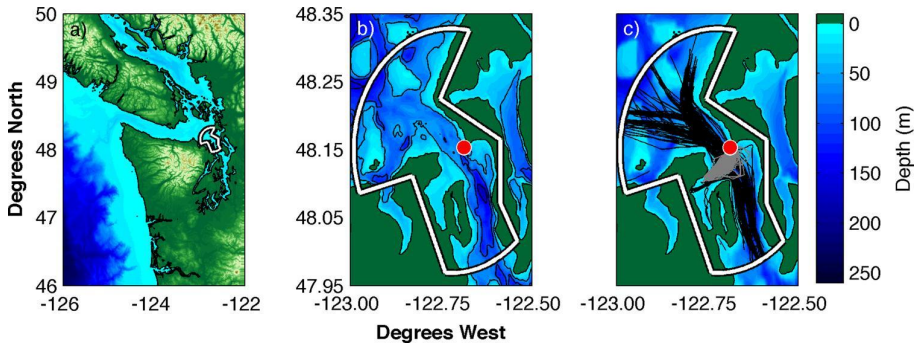

FIG. 1. (Color online) (a) The Salish Sea with the study area highlighted. (b) Admiralty Inlet bathymetry and deployment site (closed circle) with extent of ship tracking (white outline). (c). Ship tracks from January 1 to January 15, 2011. Gray lines are local ferry traffic and black lines are all other vessel traffic.

To understand the effects noise may have on marine mammal populations, the frequency content of different noise sources should be evaluated because mammalian hearing is not uniformly sensitive to all frequencies and different species have different hearing ranges. On the basis of available audiograms, Southall *et al.* (2007) proposes a weighting function or "M-weighting" for five groups of marine mammals based on functional hearing ranges to better quantify sound exposure for predicting auditory injury and other exposure effects in these animals. The five functional hearing groups are low-frequency cetaceans (baleen whales), mid-frequency cetaceans (toothed whales and most oceanic dolphins), high-frequency cetaceans (porpoises, river dolphins, and other small cetaceans), pinnipeds (seals, seal lions, and walruses) in water, and pinnipeds in air. Southall *et al.* note that these weighting functions are precautionary and, in some cases, are likely to overestimate the sensitivity of individuals. The four functional hearing groups relevant to this study are low-frequency cetaceans, mid-frequency cetaceans, high-frequency cetaceans, and pinnipeds in water.

Noise budgets quantify the relative contributions of different sources to ambient noise levels. Ambient noise is typically defined as the background noise attributed to natural physical processes and, increasingly, anthropogenic sources (Dahl *et al.*, 2007). Some definitions exclude identifiable sources such as individual vessels (NRC, 2003). Because vessel traffic is ubiquitous in busy coastal areas, the former definition (including individual vessels) is adopted for this study. In the case of shipping traffic, the National Research Council suggests identifying the contributions of unique vessel types over different temporal and spatial scales (NRC, 2003; Southall, 2005). Such information is needed to assess the impact of vessel noise on marine mammals in coastal waters, which often serve as critical habitat. Hatch *et al.* (2008) undertook a study of vessel noise and estimated a vessel noise budget for the Stellwagen Bank National Marine Sanctuary (SBNMS) to better understand the effect this noise might have on endangered North Atlantic right whales (*Eubalaena glacialis*). A similar methodology is applied to develop a vessel noise budget for Admiralty Inlet, Puget Sound, WA (Fig. 1). This study varies from Hatch *et al.* (2008) in that it considers frequencies up to 30 kHz rather than an upper limit of 1 kHz. Furthermore, this study treats anthropogenic noise in a biologically specific manner by comparing M-weighted statistics to unweighted broadband noise statistics.

II. STUDY SITE

The site consists of contiguous waters within a 20 km radius of a point 700 m to the southwest of Admiralty Head. The area serves as important habitat for a number of marine species. Specifically, Admiralty Inlet is designated as critical habitat for Southern Resident killer whales (*Orcinus orca*) (NMFS, 2006) and is regularly used by a number of other marine mammal species, including gray whales (*Eschrichtius robustus*), harbor porpoise (*Phocoena phocoena*), and Steller sea lions (*Eumetopias jubatus*). It is also an important migratory corridor for several fishes, including endangered salmonids. Admiralty Inlet is the primary inlet to Puget Sound, separating the Main Basin from the Strait of Juan de Fuca, and is 5 km wide at its narrowest point. The passage provides shipping access to the ports of Seattle, Everett, and Tacoma, as well as a number of U.S. Navy and Coast Guard facilities (e.g., Puget Sound Naval Shipyard, Bangor Submarine Base). Passenger ferries, serving as a transportation link between coastal communities, and cruise ships also make regular transits in the study area.

This research provides context for understanding existing underwater noise levels in Puget Sound and what potential further increases could result from additional development of the region's coastal waters. Particularly, Admiralty Inlet is a candidate for tidal energy development and potential impacts to marine species are under consideration. Information about the contribution of vessel traffic to the noise budget can inform the assessment of potential acoustic effects of tidal turbine installation, operations, and maintenance.

Van Parijs *et al.* (2009) note that the descriptive spatial scales, typically used in atmospheric sciences and oceanography, can be applied to studies of ecology. With respect to acoustics, the scales can be related to the distances over which species vocally communicate with conspecifics. The study area encompasses 562 km^2 of the Salish Sea, and, in accordance with the spatial scales outlined by Orlanski (1975), constitutes a mesoscale vessel noise budget.

III. METHODS

A. Acoustics data

Autonomous hydrophones positioned 1 m above the seabed were used to collect acoustic data. The hydrophones were deployed on a fixed tripod at a depth of approximately

60 m. All deployments were within 45 m of the coordinates 48.1530°N, 122.6882°W. The acoustic recording system consisted of a self-contained data acquisition and storage system (Loggerhead Instruments DSG, Sarasota, FL) with a hydrophone (HTI-96-Min) and internal preamplifier. The hydrophone had an effective sensitivity of −166 dB re μPa V^{-1}. Digitized 16 bit data were written to a Secure Digital (SD) card. For ambient noise analysis, data were obtained during four deployments of three months duration (from May 7, 2010 to May 9, 2011). The sampling frequency was 80 kHz on a 1% duty cycle (7 s continuous recording every 10 min). A shorter deployment (from February 10 to February 21, 2011), sampled at 80 kHz on a 17% duty cycle (10 s at top of each minute), was used to estimate acoustic source levels for different vessel types. Data from all deployments were analyzed from 20 Hz to 30 kHz. Throughout this document, decibels are referenced to 1 μPa.

Each recording was post-processed into windows containing 65 536 (2^{16}) data points with a 50% overlap. Windows were detrended, weighted by a Hann function, and a fast Fourier transform was applied. Resulting spectra were then scaled to preserve total variance. Variable frequency-band merging was applied on a decadal basis to produce smooth, well-resolved spectra with high confidence. The frequencies, number of merged bands, resulting bandwidth, and the equivalent degrees of freedom of the spectra are included in Table I.

Daily, hourly, and monthly statistics for unweighted broadband sound pressure levels (0.02–30 kHz) and M-weighted levels were calculated using hydrophone recordings collected between May 7, 2010 and May 1, 2011. For each calculation, recordings were split into subsets representing the statistical value of interest. For example, statistics for the hour of 01:00 to 02:00 were calculated by identifying all recordings taken between these hours over the course of the year. The mean representing the hour from 01:00 to 02:00 was obtained by averaging all recordings included in that subset. For all temporal statistics, M-weighted values for the four marine mammal functional groups (low-, mid-, and high-frequency cetaceans; pinnipeds in water) were also calculated. Temporal statistics were calculated in local time to account for daily patterns associated with scheduled vessel traffic (e.g., ferries operate on local time).

Cumulative probability distribution functions were calculated by binning unweighted and M-weighted broadband sound pressure levels. The distributions were obtained by defining discrete sound pressure level bins, identifying the number of weighted and unweighted recordings below the defined upper threshold for each bin, and normalizing the results by the total number of recordings in the analysis. The cumulative probability distribution functions highlight the overall temporal distribution of noise level statistics. A modeled cumulative probability distribution of unweighted broadband sound pressure levels was compared with the measured distribution.

TABLE I. Merged frequency bands.

Frequency (kHz)	0.01–0.1	0.1–1	1–10	10–30
Merged bands	0	3	19	41
Δf (Hz)	1.2	3.7	23.2	50.0
Degrees of freedom	10	30	190	410

B. Current measurements

Peak tidal currents in northern Admiralty Inlet exceed 3.0 m s^{-1} (Thomson *et al.*, 2012). When strong currents flow over the hydrophone, the turbulent pressure fluctuations are recorded by the hydrophone as additional noise. These pressure fluctuations, often referred to as pseudosound or flow-noise, are non-propagating and are of sufficient intensity to mask propagating noise sources including large ships (Lee *et al.*, 2011). Because pseudosound is non-propagating, it should not be included in the noise budget. In addition, when depth-averaged currents exceed 1 m s^{-1}, noise levels increase with current at frequencies greater than 2 kHz. These increases are consistent with the mobilization of gravel, small cobbles, and shell hash (Thorne *et al.*, 1984; Thorne, 1990).

Acoustic recordings with depth-averaged currents exceeding 0.4 m s^{-1} were excluded from this analysis to prevent biasing the statistics with pseudosound, which also excludes propagating ambient noise from bedload transport. These periods were identified using co-spatial velocity records from an Acoustic Doppler Current Profiler (470 kHz Nortek Continental, Nortek AS, Vangkroken, Norway). Current profiles were calculated in 1 m bins using 10 min ensemble averages.

To verify that excluding periods with strong currents from analysis was not likely to bias statistics related to vessel noise, an average vessel presence was calculated in 0.1 m s^{-1} velocity bins for all current data. In each bin, a summation of all recorded vessel minutes was normalized by the total number of minutes during which currents in each bin were recorded. The results were compared to justify the assumption that vessel presence was independent of currents.

C. Automatic Identification System data

Automatic Identification System (AIS) transponders are used as a real-time collision avoidance tool and are mandated for commercial maritime vessels exceeding 300 gross tons, tugs and tows, and passenger ships (Federal Register, 2003). Although not required, some recreational vessels are also equipped with the AIS transponders. AIS transponders transmit very high frequency radio signals, referred to here as AIS strings, containing dynamic ship information (i.e., position, heading, course over ground, and speed over ground) up to twice per second while a vessel is in transit. Static information, including but not limited to ship name, type, length overall, draft and destination are transmitted every 6 min while in transit. A unique Maritime Mobile Service Identity (MMSI) number is transmitted with both static and dynamic data.

AIS transmissions were logged by a receiver (Comar AIS-2-USB, Comar Systems Ltd., Cowes, UK) on the Admiralty Head Lighthouse at Fort Casey State Park, WA, approximately 1 km from the hydrophone deployment site.

The receiver was connected to a data acquisition computer running a PYTHON script to record all incoming AIS strings and append time stamps. In post-processing, a PYTHON package (NOAA data version 0.43) (Schwehr, 2010) converted all received AIS transmissions into an array of text data for further manipulation. For each received AIS string with dynamic data, the MMSI number, speed over ground, course over ground, and vessel coordinates were stored. Static information including the vessel length overall, vessel name, and vessel type were recorded in a look-up table containing information about all vessels recorded in the study area.

The vessel coordinates from the processed AIS strings containing dynamic ship information were used to calculate a radial distance between the ship and the hydrophone (given a water depth of approximately 60 m, the radial distance and slant distance were nearly equivalent for most transmissions). Dynamic AIS information for each vessel in the study area at any time was averaged over 1 min periods. Data were filtered to include only those AIS transmissions from vessels under way (speed over ground greater than 0.1 kn) within the geographic area outlined in Fig. 1. Transmission/receipt of implausible local coordinates (latitude $> 90°$, longitude $> 180°$) occurred infrequently and has been noted in other studies (e.g., Harati-Mokhtari *et al.*, 2007).

Records of MMSI numbers, ship types, and ship lengths were compared against online public information. Using vessel names, information was found by searching a registered vessel database in the United States or other available online fleet information.[1] To the greatest extent possible, unknown and incorrect ship types were corrected to accurate values, unrealistic speeds over ground removed, incorrect ship lengths updated, and records with invalid MMSI numbers excluded through manual analysis.

The vessels were separated into four broad categories, as defined by their AIS vessel codes—"commercial" (AIS codes 70-89, 30-32, 52), "passenger" (60-69), "other" (90-99), and "various" (all other codes). Within the commercial category, vessels were further separated by AIS vessel code into cargo ships (AIS code 70-79), tankers (80-89), tugs (31, 32, 52), and fishing vessels (30). The cargo category was subdivided into four different vessel types, using their MMSI numbers, emphasizing differences in vessel design related to the type of transported good. The four cargo types include container vessels, vehicle carriers, general cargo vessels, and bulk carriers. The cargo type for each vessel was determined by cross-checking the vessel name with available fleet information. Throughout the rest of the document, references to cargo vessels include the four types within this category unless otherwise noted.

Within the passenger category, vessels were separated by MMSI into local passenger ferries, cruise ships, and "passenger other" for vessels that do not fit into the first two passenger vessel designations. As for cargo vessels, this categorization was motivated by the presence of vessels with the same AIS vessel code, but different design characteristics. For example, a small whale-watching vessel (length overall <20 m) and a cruise ship both used AIS code 60 while their expected source levels varied significantly. The category "various" was used to combine uncommon ship types (e.g., underwater operations vessels and anti-pollution equipment) and ship types underrepresented by AIS statistics (e.g., military vessels and pleasure craft). The vessel code "other," an AIS designation, was used by vessels that have no formal designation that fits within another class (e.g., research vessels).

The average and standard deviations of the speed over ground and length overall were determined for each type. These metrics were calculated directly from all 1 min averaged data associated with each type. By this method, slow moving vessels contributed more points to the statistics, potentially biasing the statistics toward the speeds and lengths of the slower vessels. However, the statistics calculated using this method were similar, within 3 kn of speed over ground and 10% of the length overall, to distance-weighted statistics for all vessel types but ferries. For ferries, the statistics were different due to a distribution dominated by a set of small, faster moving ferries and a larger, slower moving ferry.

To visualize vessel traffic, average location data for each 1 min period were gridded into 100 m bins and the total number of minutes of vessel presence in each bin calculated by vessel type. Opportunistic sightings of vessels not transmitting AIS data (e.g., military vessels) served to inform the interpretation of results but were not included in the analysis.

The AIS data acquisition system was intermittently inactive for approximately 42 days (11% of the year) due to power failures and hardware malfunctions. All statistics and calculations were based on received data and no attempt was made to extrapolate the data to account for receiver outages.

D. Acoustic and AIS data integration

Data from the higher duty cycle deployment (from February 10 to February 21, 2011) were used to estimate the source levels for three vessel types. Acoustic and AIS data were combined and source levels (SL) were backcalculated using the received levels (RL) and the sonar equation. The acoustic source level represents the sound pressure level (SPL) at a nominal distance of 1 m from the source, although for a large, multi-point source such as a cargo vessel, this quantity is an abstraction. Transmission losses account for geometric spreading of an acoustic wave and losses associated with boundaries and attenuation. At low frequencies (<1 kHz), where most of the energy from large commercial ship traffic is contained, and at the spatial scales considered in this study, attenuation effects from seawater are negligible (Ainslie and McColm, 1998). Source levels were calculated by

$$\mathrm{SL} = \mathrm{RL} + N \log_{10}(r), \tag{1}$$

where N was the transmission loss coefficient and r was the radial distance between vessel and hydrophone in meters, as determined from AIS position data. Source levels for individual ships were calculated from received level data at the closest point of approach (CPA). We used a transmission loss coefficient of 15, a value justified by range dependent

parabolic equation (PE) modeling of sound propagation at key frequencies at the site (Appendix A). When no AIS-equipped vessels were within the study area, a received level of 100 dB was assumed, a value consistent with the lowest recorded broadband SPLs (0.02–30 kHz) at the site.

For each type of vessel, the total amount of time spent in the survey area (vessel hours) was determined from the AIS data. The energy inputs to the vessel noise budget were calculated for each vessel type on the basis of an assumed source level and time spent within the study area. The assignment of source levels to vessel classes is discussed in Sec. IV C. Source levels, in watts, were converted to power by

$$\mathrm{SL}\,[\mathrm{W}] = \frac{A\,p^2}{\rho\ c} = 4\pi\frac{\left(10^{-6}\times 10^{(\mathrm{SL[dB]}/20)}\right)^2}{\rho\ c}, \tag{2}$$

where A was the area of a 1 m sphere surrounding the idealized source, and the SL on the right-hand side was in units of dB re μPa at 1 m. Because of the strong currents over the Admiralty Inlet sill, the water column is generally well-mixed with minimal stratification (Polagye and Thomson, 2010) so a constant sound speed ($c = 1490\,\mathrm{m\,s^{-1}}$) and density ($\rho = 1024\,\mathrm{kg\,m^{-3}}$) were appropriate for this location. The energy budget was calculated by combining the source power output and the total amount of time spent by a given vessel type in the study region according to

$$E\,[\mathrm{J}] = \sum_{j=1}^{n} \mathrm{SL}_j[\mathrm{W}]t_j[\mathrm{s}], \tag{3}$$

where E was the energy budget in joules, SL was the source level in watts, t was the time interval, and j was the index for the vessel.

The contribution of vessels to ambient noise was calculated using a first-order reconstruction of received noise levels based solely on information about vessel locations, vessel types, and characteristic source levels. One minute averaged AIS data and estimates of vessel source levels were used to model the received levels at a given time by

$$\mathrm{RL}(t)\ [\mathrm{dB}] = 10\log_{10}\left(\sum_{k=1}^{n}\left(\frac{10^{\mathrm{SL}_k\ [\mathrm{dB}]}}{r_k^N}\right)^{1/10}\right), \tag{4}$$

where RL(t) was the modeled received level during time interval (t), n was the total number of vessels in the area interval during the time interval, SL_k was the source level, r_k was the horizontal distance between the receiver and vessel k (of known class), and N was the single-valued transmission loss coefficient of 15. Regions within 500 m of the local ferry docks on either side of Admiralty Inlet were excluded due to the rapid decrease in source level as the ferry approached the dock. This model presumes that aggregate vessel noise is given by the incoherent addition of multiple vessel sources. The summation was calculated for each 1 min interval to produce a time series of reconstructed received levels attributable to vessels. These were compared to received level statistics derived from hydrophone recordings over the same time period to estimate the contribution of vessel noise to the ambient noise budget.

An energy flux cumulative probability distribution function was constructed by converting the received levels in decibels to acoustic intensities (linear scale), and multiplying the acoustic intensities by the amount of time they are observed. The energy flux distribution was used to compare the contribution of acoustic energy flux from vessels to the total acoustic energy flux measured by the hydrophone.

As discussed in Sec. III B, periods with strong currents ($>0.4\,\mathrm{m\,s^{-1}}$) were excluded from ambient noise analysis to remove the effects of pseudosound. This is a conservative restriction and only 18.4% of the data (8856 recordings) satisfied this criterion. Analysis of bin-averaged vessel presence showed that there were, on average, approximately 2.5 vessels in the study area at any given time. Vessel presence was approximately constant during the lowest 95% of the measured current velocities. During the strongest currents

TABLE II. Ship traffic summary, including the total number of vessels, the total number of vessel hours spent in the study area, average speed over ground, and average length overall by vessel class and type. SOG and LOA values include the standard deviations.

Vessel class	Vessel type	Number of vessels	Vessel hours[a]	SOG (kn)	LOA (m)
Commercial	Container	237	2113	20.1 ± 2.6	264 ± 48
	Vehicle carrier	123	611	18.8 ± 2.9	212 ± 35
	General cargo	35	292	12.4 ± 3.1	121 ± 59
	Bulk carrier	208	755	13.5 ± 2.0	206 ± 23
	Oil/chemical tanker	31	240	14.1 ± 2.4	206 ± 49
	Tug	212	8502	7.7 ± 2.9	29 ± 13
	Fishing	259	1577	9.3 ± 2.8	46 ± 25
Passenger	Ferry	19	3868	13.7 ± 7.8	72 ± 21
	Cruise	22	551	16.4 ± 3.7	248 ± 63
	Other	15	75	8.8 ± 5.1	30 ± 14
Other	—	30	330	9.4 ± 4.2	55 ± 52
Various	—	173	1184	10.8 ± 5.5	63 ± 57
Total		1364	20 100		

[a]AIS system operated for 7761 h during the year. Two vessels in the study area during the same time interval count as two vessel minutes.

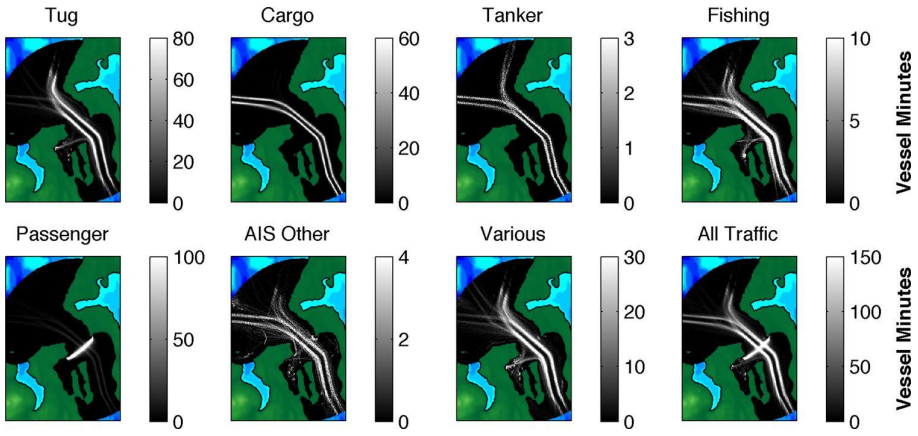

FIG. 2. (Color online) Ship traffic density map plotted on a 100 m × 100 m horizontal grid. Each subplot represents an area with the dimensions of 28 km by 40 km. In the passenger vessel density subplot, grid points located under the ferry traffic route are saturated to avoid obscuring the traffic patterns of other passenger vessels such as high-speed ferries.

($>2.3\,\mathrm{m\,s^{-1}}$), overall vessel presence decreased to 1.8 vessels. Given that mean vessel presence across velocity bins was constant, with only modest decreases when currents exceeded the 95th percentile, we concluded statistics were not biased by the exclusion of data due to pseudosound.

IV. RESULTS

A. Vessel traffic

Over the 1 year period (May 1, 2010–May 1, 2011), a total of 1376 unique vessels were recorded in the study area. Of this total, only 13 were unidentified due to invalid MMSI numbers. Based on overall presence, tugs, passenger ferries, and container ships were the most common vessel types. Other large commercial vessels, including vehicle carriers and bulk carriers, were also common. An AIS-transmitting vessel was found to be present within the study area 90% of the time, and multiple vessels were present 68% of the time. The number of unique vessels and the total number of hours spent in the survey area, by type, are included in Table II. Also included are the average and standard deviations of speed over ground (SOG) and length overall (LOA). Cargo ships, especially vehicle carriers and container ships, transit the study area at higher speeds than the other types of commercial traffic. The fast moving vessels elevate received levels at the hydrophone site for up to 30 min, while slower moving vessels elevate received levels for up to 60 min.

Vessel density maps by type (Fig. 2) are used to visualize the temporal and spatial distributions of ships contributing to the noise budget during the study period. Each vessel density plot is presented with a unique color scale to avoid saturation and provide details that would not appear if common colorbar axes were used. Vessel traffic regulations result in limited spatial variability for traffic patterns, with most commercial vessels present in the designated traffic lanes passing through the middle of the inlet. Cargo ships generally arrive from or are bound for the open waters of the Pacific Ocean, while tanker and tug traffic typically transits along the inland Washington coast. Fishing vessels and those classified as "other" or "various" are less likely to utilize the shipping lanes while transiting the study area. The passenger vessel map clearly demonstrates that the local ferry route dominates the passenger vessel density map, although ferries en route to Victoria, BC and cruise ships en route to Alaska are also evident.

B. Ambient noise

Broadband and one-third octave band SPLs for 12 h provide important detail on how ambient noise levels vary at the study site (Fig. 3). For example, increased noise levels below 50 Hz correspond to pseudosound (velocity $\approx 0.5\,\mathrm{m\,s^{-1}}$) at the hydrophone between 0 and 1.5 h. Unique spectral characteristics associated with individual vessel passages are also present during this 12 h recording and correspond to AIS ship tracks (Fig. 3; Table III). The maximum broadband SPL observed during the 12-h period, 140 dB re 1 μPa, corresponds to the passage of a container ship in the southbound shipping lane at a range of 2.7 km (CPA 1 in Fig. 3; Table III). In general, the largest increases in received levels are concentrated at frequencies less than 1 kHz. However, these are broadband events, with acoustic energy increasing in all one-third octave bands (center frequency up to 25 kHz).

The cumulative probability distribution functions for SPLs are shown in Fig. 4 on a broadband (unweighted) and

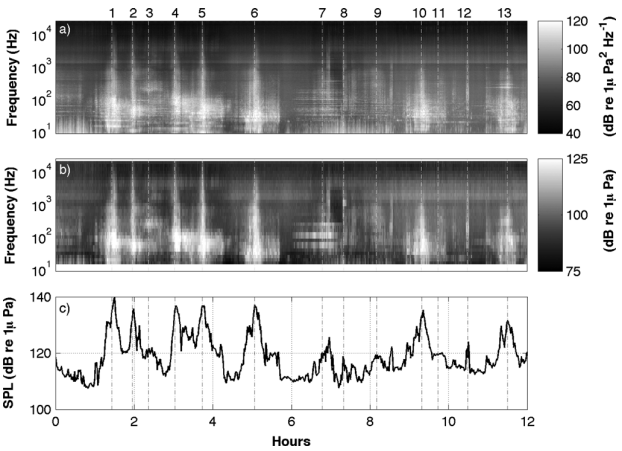

FIG. 3. Sample acoustic data from February 12, 2011. The time series are constructed from 10 s recordings every minute. (a) Spectrogram showing regular increases in energy content over all frequencies due to vessel traffic. (b) Time series of one-third octave band SPLs with center frequencies from 16 Hz to 25 kHz. (c) Time series of broadband SPLs (0.02–30 kHz).

TABLE III. Vessel name, type, LOA, SOG, and CPA for events highlighted in Fig. 3.

Name	Vessel type	LOA (m)	SOG (kn)	CPA (km)
1 Manoa	Container	261	23.4	2.7
2 Horizon Kodiak	Container	217	20.5	1.5
3 Norma H	Tug	24	7.2	2.9
4 Hong Yu	Bulk carrier	226	13.8	1.5
5 Great Land	Vehicle carrier	243	22.9	1.4
6 Zim Chicago	Container	334	21.1	2.7
7 Chetzemoka	Ferry	83	10.7	2.4
8 Chetzemoka	Ferry	83	9.5	1.2
9 Henry Sause	Tug	33	9.3	3.0
10 Xin Ri Zhao	Container	263	20.9	2.6
11 Ocean Mariner	Tug	29	5.0	2.8
12 Chetzemoka	Ferry	83	12.5	1.3
13 Ever Excel	Container	300	18.5	2.8

M-weighted basis. The mean broadband SPL at the site is 119.2 ± 0.2 dB (95% confidence interval). Statistics for received M-weighted levels are influenced by the sensitivity of the functional groups to different frequencies. That is, low-frequency cetaceans have the most sensitive hearing at frequencies overlapping peak source levels from vessel traffic. Therefore, M-weighted levels for low-frequency cetaceans are similar to the measured distribution. For the other functional groups, M-weighted received levels decrease corresponding to the decreased sensitivity in the range of peak levels from vessel traffic. For high-frequency cetaceans, the functional group least sensitive to low-frequency noise, mean M-weighted SPLs are approximately 5 dB lower than the mean for low-frequency cetaceans.

Hourly, daily, and monthly mean broadband SPLs and ranges for the percentile statistics are shown in Fig. 5. Diurnal patterns are primarily attributed to the absence of ferry traffic and periodic lulls in commercial shipping at night. Monthly averages are highest during the summer, in part due to cruise ship traffic. High average noise levels in January, when compared to December and February, are a result of higher levels of commercial ship traffic during the typically less noisy periods in the late evening and early morning. Measured noise levels are comparable to reported values from Haro Strait off of the west coast of San Juan Island, WA (USA) (Veirs and Veirs, 2005). Broadband SPLs (0.1–15 kHz) at that location were 117.5 dB during the summer and 115.6 dB throughout the rest of the year. In Admiralty Inlet, the mean broadband SPL calculated over the same frequency range for the entire year in the current study was 116.2 ± 0.2 dB (95% confidence interval).

Received level percentile statistics of pressure spectral densities, broadband SPLs, and one-third octave band SPLs were derived from cumulative probability distributions. Figure 6 shows the percentile spectra associated with the broadband received levels. One-third octave band SPLs are nearly constant, around 90 dB from approximately 100 Hz to 20 kHz, during least noisy periods. The largest variations in energy content ($f < 1$ kHz) are consistent with commercial ship traffic. A spectral peak at approximately 1.5 kHz was regularly identified in data sets from the site and is approximately 6 dB higher than adjacent frequencies. The peak scales with the energy in the acoustic spectrum (i.e., there is a 6 dB peak at 1.5 kHz relative to both the 5% and 95% spectra). This feature is consistent with constructive interference

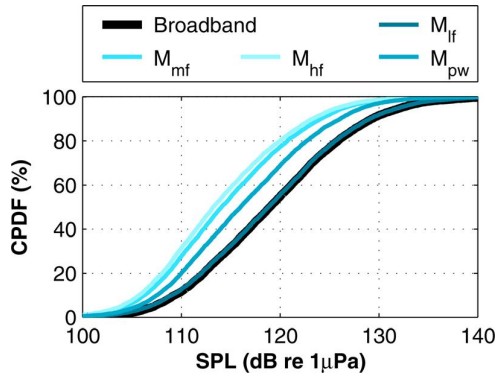

FIG. 4. (Color online) Cumulative probability distribution function of unweighted broadband SPLs (0.02–30 kHz) and M-weighted cumulative probability distribution functions for pinnipeds in water (M_{pw}) and low- (M_{lf}), mid- (M_{mf}), and high-frequency (M_{hf}) cetacean marine mammal functional hearing groups.

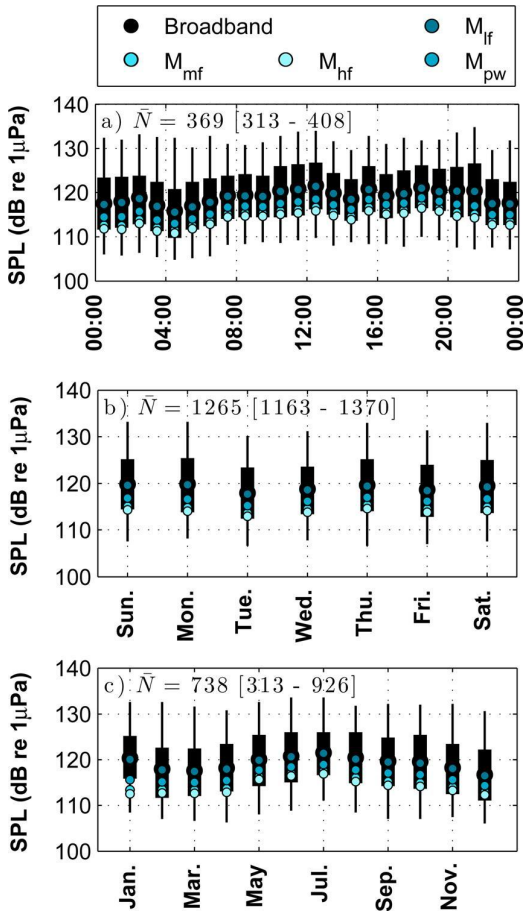

FIG. 5. (Color online) Hourly (a), daily (b), and monthly (c) average broadband (0.02–30 kHz) and M-weighted SPLs. The box plots show the range for the 25%–75% thresholds and the whiskers show the range for the 5%–95% thresholds for broadband SPLs. The mean, minimum, and maximum sample sizes ($\bar{N}$) are included for the statistics in each subplot. February and August sample sizes were significantly below the mean due to extended AIS receiver outages and data gaps from bottom-package recovery/redeployment.

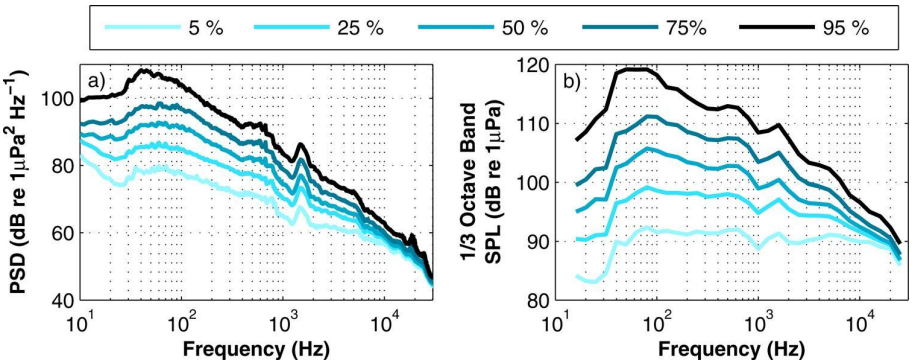

FIG. 6. (Color online) (a) Percentile calculations of pressure spectral density for unweighted received levels. (b) Percentiles for unweighted received levels in one-third octave band SPLs. The received broadband SPLs associated with the percentage thresholds are 107.3 dB (5%), 113.4 dB (25%), 119.2 dB (50%), 124.5 dB (75%), and 132.3 dB (95%).

near the seabed since the corresponding wavelength of the peak is 1 m, the same distance as between the hydrophone and the seabed.

C. Vessel source levels and energy budget

A combination of site-specific data and literature values was used to attribute source levels to vessel types. The energy budget and received level model in this study are most sensitive to the source levels of cargo ships, tugs, and ferries due to their relative presence. Less common vessel types in this study show significant variability in length and SOG. Therefore, choosing a characteristic source level for the less common vessel types is difficult. Since the literature is limited the approach used here to assign source levels is, by necessity, *ad hoc*, with all source level assumptions described in the following section.

The validity of applying a single-valued transmission loss coefficient to estimate source levels based on Eq. (1) is contingent on its accuracy at key frequencies of vessel noise. Figure 7 includes example spectra for a cargo ship, the local ferry, and a tug at their CPA. In the received spectra from the closest points of approach, peak spectrum levels occur well below 1 kHz. Based on these spectra, PE modeling of propagation to justify the use of the single-value transmission loss coefficient was carried out at 50, 100, and 250 Hz (Appendix A).

Source level estimates for different vessel types at the their closest points of approach are shown in Table IV. Source levels are only presented for periods when currents are relatively weak (to minimize pseudosound) and when spectra are not contaminated by other ships. Because these are uncommon events at the study site, it is not possible to estimate source levels for all vessel types in Admiralty Inlet.

Given the agreement in average LOA and SOG values, it is unsurprising that sources levels for cargo ships reported in the current study are representative of values reported by others (e.g., McKenna *et al.*, 2012). Specifically, the source levels applied in the current study are 186 dB for container ships, 180 dB for vehicle carriers, 180 dB for general cargo ships, 185 dB for bulk carriers, and 181 dB for oil and chemical tankers. The consistency of calculated source levels also supports the use of a single-valued transmission loss coefficient for this study area.

Different source levels are applied to each type of passenger vessel. Although the ferry category includes 19 vessels, the local ferry is temporally dominant. A source level of 173 dB is used for ferry traffic and is based on recordings of local ferry traffic during the 1 year deployment (Appendix B). A source level of 180 dB is assigned to cruise ships that depart from Seattle for Alaska during the summer months. This value is consistent with the source level applied by Hatch *et al.* (2008) and measurements made of two large cruise ships at the U.S. Navy's Southeast Alaska Acoustic Measurement Facility (SEAFAC) in Ketchikan, AK (Kipple, 2004a,b). The remaining passenger vessels are, on average, smaller than the local ferry and cruise ships and spend less time in the study area. A lower source level of 165 dB is attributed to the remaining passenger vessels. This source level value is between large commercial vessels and small recreational watercraft and is comparable to source levels reported for small commercial vessels and larger recreational vessels (Greene and Moore, 1995; Kipple and Gabriele, 2003).

Tugs transiting the study site span a broad range of sizes and tow loads. Broadband source levels for tugs reported in literature include 170 dB (Greene and Moore, 1995) and 172 dB (Hatch *et al.*, 2008). A source level of 172 dB for

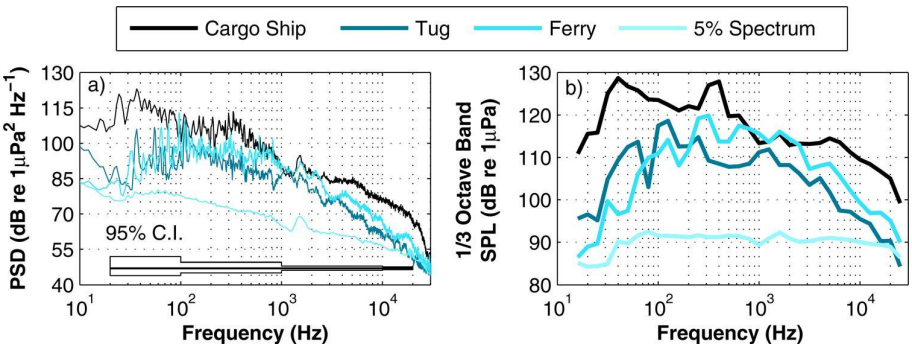

FIG. 7. (Color online) (a) Acoustic spectra for a cargo ship at 1.5 km, the local ferry at 1.0 km, and a tug at 1.2 km, and the fifth percentile spectrum. (b) One-third octave band SPLs for the respective spectra in (a).

TABLE IV. Estimated source levels (0.02–30 kHz) based on received levels (0.02–30 kHz) for selected ships.

Date/time	Name	Vessel type	LOA (m)	SOG (kn)	CPA (km)	RL (dB)	SL (dB)
February 15, 2011 9:20	Victoria Clipper IV	Ferry	36	30.8	1.65	121	170
February 16, 2011 9:18	Victoria Clipper	Ferry	40	30.5	1.26	121	168
February 13, 2011 6:51	Eagle	Tug	32	9.6	1.22	127	173
February 16, 2011 4:41	Valor	Tug	30	8.4	1.46	121	168
February 16, 2011 12:25	Lela Joy	Tug	24	4.9	1.15	126	172
February 15, 2011 4:14	Pacific Eagle	Tug	28	8.2	1.36	118	165
February 20, 2011 18:28	Shannon	Tug	28	9.3	0.58	129	171
February 11, 2011 23:30	James T Quigg	Tug	30	7.9	1.42	120	167
February 19, 2011 6:23	Island Scout	Tug	30	5.8	1.47	127	174
February 20, 2011 12:44	Chief	Tug	34	11.4	1.23	128	174
February 12, 2011 1:57	Horizon Kodiak	Container	217	20.1	1.53	132	179
February 12, 2011 3:02	Hong Yu	Bulk carrier	226	13.6	1.52	135	182
February 12, 2011 3:44	Great Land	Vehicle carrier	243	23	1.36	137	184
February 12, 2011 11:30	Ever Excel	Container	300	18.2	2.78	132	183
February 14, 2011 7:42	Ever Excel	Container	300	20.8	1.93	136	186
February 12, 2011 22:24	Hanjin Hamburg	Container	335	23.8	2.82	133	185
February 14, 2011 2:39	Hanjin Hamburg	Container	335	21.3	1.51	137	185
February 14, 2011 9:02	CSK Unity	Bulk carrier	225	13.6	2.07	128	178
February 14, 2011 19:07	CMA CGM Carmen	Container	334	23.8	1.46	136	183
February 14, 2011 19:56	MSC Kim	Container	265	22.7	1.35	136	183
February 16, 2011 9:00	Bremen Bridge	Container	279	21.2	1.02	136	181
February 17, 2011 7:53	Hyundai Republic	Container	305	24.7	1.49	136	184
February 17, 2011 22:34	Coastal Sea	General cargo	55	12.5	1.36	129	176
February 21, 2011 0:14	Green Point	Vehicle carrier	180	19.1	1.41	133	180

tugs, the average value (in root-mean-square pressure space) for all tugs shown in Table IV, is used. Source levels for the remaining ship types are broken into three categories—fishing, other, and various. A source level of 165 dB is used for fishing vessels and is based on one-third octave band spectra of trawlers and small vessels with diesel engines (Greene and Moore, 1995). A source level of 165 dB is also used to calculate noise budget contributions from the remaining vessel classes (various and other). These categories include a broad range of vessel types and sizes. However, the energy budget is insensitive to errors in source levels for these vessel categories because of their limited presence in the study area.

The total acoustic energy input of vessel traffic equipped with AIS in the study area over the course of the year (Table V) is 438 MJ. Commercial vessel traffic accounts for over 90% of the energy budget with container vessels being the greatest contributor due to high source levels. Despite relatively low source levels, tugs are large contributors to the energy budget due to their relative presence. Passenger ferries and cruise ships represent 9% of the total energy budget. Notably, the energy input from cruise ships is mostly limited to the summer tourist season. When compared to shipping vessels, tugs, and passenger vessels, energy input from all other vessel types is negligible.

The cumulative probability distribution functions for the modeled and observed noise are presented in Fig. 8. Above the 15th percentile, the measured noise distribution falls within the model results for the $N = 15$–16 envelope [Eq. (4)]. The good agreement between measured and modeled results suggests that most of the ambient noise variability at the site can be explained by AIS-equipped vessel traffic. During quieter periods, other noise sources, such as distant shipping, wind, and waves, are likely to dominate. Limited land-based commercial and industrial activity in the immediate vicinity of the study area also suggests that noise from other anthropogenic sources is insignificant. Based on temporal variability explained by vessel traffic in Fig. 8, a cumulative energy flux distribution (not shown) reveals that vessels traffic accounts for 99% of the acoustic energy flux at the measurement location.

V. DISCUSSION

A. Energy budget

The sensitivity of the energy budget depends primarily on the source levels assigned to cargo ships, tugs, and passenger vessels due to their temporal dominance. For each 1 dB increase in source levels attributed to tugs and ferries, the total energy added to the budget increases by 10 MJ (2%) and 3 MJ (<1%), respectively. Because these three vessel types spend an order of magnitude more time in the study area than others, the total budget is relatively insensitive to source levels attributed to traffic of other vessel types (with the exception of fishing vessels). Therefore, proper attribution of source levels for less common vessel types, while desirable, is relatively unimportant.

AIS data are a useful tool for quantifying the densities of commercial and passenger vessel traffic. However, small recreational watercraft and fishing vessels, neither of which is required to use AIS, are also common in the area. The vessel noise budget does not include the contribution from vessels without AIS transponders, and this is a notable limitation if relying on AIS as the sole source of vessel traffic data.

TABLE V. Vessel noise budget calculated by Eq. (3).

Vessel class	Vessel type	SL (dB)	SL (W)	Time (h)	Energy (MJ)	% of Budget
Commercial	Container	186	32.8	2113	249	57
	Vehicle carrier	180	8.2	611	18	4
	General cargo	180	8.2	292	9	2
	Bulk carrier	185	26.0	755	71	16
	Oil/chemical tanker	181	10.4	240	9	2
	Tug	172	1.3	8502	40	9
	Fishing	165	0.3	1577	1	<1
Passenger	Ferry	173	1.6	3868	23	5
	Cruise	180	8.2	551	16	4
	Other	165	0.3	75	<1	<1
Other	—	165	0.3	330	<1	<1
Various	—	165	0.3	1184	1	<1
Total				20 100	438	100

In the current study, many fishing vessels are included in the vessel noise budget, but it is unclear what portion of fishing vessels are equipped with AIS. Furthermore, there is a general lack of acoustic measurements of different types and sizes of fishing vessels. Military vessels (the most common vessel type included in the "various" category), do, occasionally, transmit AIS signals but the summary contained in Table II understates the level of military traffic in the area. Based on opportunistic sightings of naval vessels in the field that are not reflected in AIS data, additional transits are known to occur. It is unclear what portion of the total military traffic is included in the budget and the question is further complicated by variations in vessel design. Given the relatively small number of vessel hours in the study area, a substantially different assumption of source level or presence for vessels classified as "various" would be required to affect the energy budget. For example, a source level of 176 dB (an 11 dB increase over the current value) or an increase in presence by 1300% for this vessel category would increase the energy budget by 1% (4.4 MJ). Recreational watercraft and small fishing vessels, although common, have lower source levels (Greene and Moore, 1995; Erbe, 2002; Kipple and Gabriele, 2003; Hildebrand, 2005, 2009) and their exclusion is unlikely to substantially influence the overall vessel noise budget. For example, if a broadband source level of 155 dB is assumed for all recreational watercraft, these vessels would need to spend 47 000 h in the study site per year, more than two times the combined vessel presence of all types in this study, to increase the vessel energy budget by 1%.

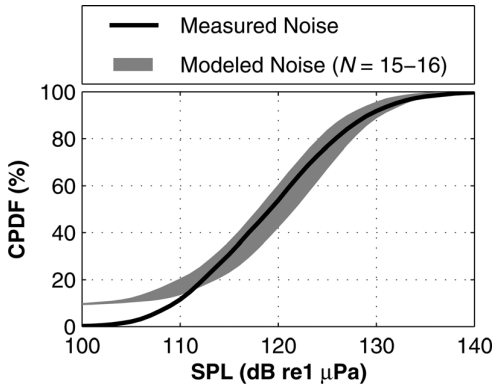

FIG. 8. Cumulative probability distributions of ambient noise (0.02–30 kHz) in the study area for measurements (all ambient noise sources) and the model for vessel noise. The gray envelope of modeled noise represents predicted received levels using transmission loss coefficients from 15 to 16.

An energy budget for vessel noise is useful for identifying the relative contributions of different types of vessels to ambient noise levels, but site-to-site comparisons of the absolute budget are difficult. Comparisons may be possible if the energy budgets are normalized by the study area. The total study area for Admiralty Inlet is 562 km^2 and the resulting vessel noise energy density is 0.78 MJ $km^{-2}\,yr^{-1}$. Note again that this figure has not been extrapolated to account for the 11% of the year when no AIS data were obtained due to outages. By contrast, Hatch *et al.* (2008) estimated an annual energy budget of 193 MJ in SBNMS. Using the total area of the SBNMS (2188 km^2), the spatial energy density is 0.09 MJ $km^{-2}\,yr^{-1}$, nearly an order of magnitude lower than Admiralty Inlet.

Energy budgets, although effective for measuring the relative contributions of different noise sources, are not static. Such budgets are dependent on overall levels of activity. In the case of Admiralty Inlet, most of the energy budget is related to economic activity in the form of shipping vessels and to ferry traffic. Large changes in shipping traffic at the Ports of Seattle and Tacoma would be reflected in overall energy budget. In addition, after the end of the study period, a second ferry was added to the local ferry route, so an updated energy budget would indicate higher levels of passenger vessel traffic.

B. Relevance to marine species

Behavioral responses of marine mammals to vessel noise depends not only on the RL of noise, but also on other variables, including the individual's hearing sensitivity, current activity state, and previous experience with sounds of similar intensity and frequency (Southall *et al.*, 2007; Ellison *et al.*, 2011). Most research on vessel noise has focused either on low-frequency, ocean basin scale contributions from commercial shipping traffic or small watercraft in close proximity to marine mammals (e.g., Erbe, 2002; Clark *et al.*, 2009).

Numerous studies of marine mammal reactions to vessels suggest that exposure to elevated vessel noise may alter marine mammal behavior and increase stress hormone levels with potential biological consequences (Buckstaff, 2004; Foote *et al.*, 2004; Holt *et al.*, 2009; Rolland *et al.*, 2012).

Broadband SPLs at the study site regularly exceed 120 dB [Fig. 3(c)], the current acoustic criterion for behavioral harassment of marine mammals for continuous sound types (120 dB re 1 μPa) in the United States (NMFS, 2005). The current acoustic criteria are based on broadband measurements and do not take into account frequency-specific hearing capabilities that differ among marine mammal groups. The weighted cumulative probability distributions of received levels for each marine mammal functional hearing group are shown in Fig. 3 in an effort to address variation in hearing capabilities among groups. Because low-frequency cetaceans and pinnipeds have relatively flat hearing sensitivity over the frequencies associated with commercial shipping, their received levels approach the broadband receiver idealization. However, the M-weighting functions for mid- and high-frequency cetaceans start to roll off at frequencies less than 1 kHz, where the majority of acoustic energy associated with commercial ships is concentrated. Consequently, perceived mean received levels for mid- and high-frequency cetaceans based on these weighting functions are, on average, at least 5 dB lower. As previously mentioned, noise from recreational vessels is unlikely to contribute substantially to the vessel noise budget in the study location. Nonetheless, noise from these smaller vessels may be of concern to mid- and high-frequency cetaceans because their energy is concentrated at higher frequencies than commercial ships (Erbe, 2002). This points to a general need for frameworks that are able to treat anthropogenic noise in a more biologically relevant manner.

At close range (e.g., within 10 km of the source), different types of vessel activity increase noise levels across a broader range of frequencies than is often considered. Below 1 kHz, ship traffic regularly increases noise levels by 25 dB above background levels. At higher frequencies, extending up to 30 kHz, one-third octave band SPLs regularly increase by 10–20 dB [Figs. 3(b) and 6]. These increases in ambient noise from shipping traffic are sufficient to regularly mask communicative sounds used by many marine mammals unless they are able to compensate vocally (Holt *et al.*, 2009).

Because the Main Basin of Puget Sound is also relatively narrow (approximately 10–20 km wide), large commercial vessels transiting the area are expected to elevate broadband ambient noise levels over the entire width of the channel to levels in excess of 120 dB. The hydrophone deployments in this study are well outside (>1 km) of the shipping lanes and, as shown in Fig. 1(c), few vessels passed directly over the deployed hydrophones. As a result, moderately higher recorded broadband SPLs would be expected mid-channel, where vessel densities are greater. The proximity to ferry routes, shipping lanes, and populated coastal communities are common throughout Puget Sound. Therefore, the noise levels observed in this study area may be extended, with due caution, to other areas in the region.

VI. CONCLUSION

One year of AIS data is paired with hydrophone recordings from a site in northern Admiralty Inlet, Puget Sound, WA to assess ambient noise levels and the contribution of vessel noise to these levels. Admiralty Inlet experiences a high level of vessel traffic due to cargo ships bound for major ports, tugs towing barges, and ferries transporting passengers and vehicles. Results suggest that ambient noise levels between 20 Hz and 30 kHz are largely driven by vessel activity and that the increases associated with vessel traffic are biologically significant.

Throughout the year, at least one AIS-transmitting vessel is within the study area 90% of the time and multiple vessels are present 68% of the time. A vessel noise budget is constructed to assess the relative contributions of different vessel types to underwater noise levels at the site. Results show cargo vessels account for 79% of the acoustic energy in the vessel noise budget. Passenger ferries and tugs have lower source levels but spend substantially more time in the study site and contribute 18% of the energy in the budget. Recreational watercraft contribute to ambient noise levels but are unlikely to contribute substantially to the overall vessel noise budget due to limited presence and lower source levels. All vessels generate acoustic energy at frequencies relevant to all marine mammal functional hearing groups.

A basic model for received levels accounts for vessel types, distance to the hydrophone, and specified characteristic source levels for each vessel type. The model explains 85% of the temporal variability in observations and demonstrates the predominance of maritime traffic in the overall noise budget at the site.

ACKNOWLEDGMENTS

Thanks to Joe Talbert and Alex deKlerk for their work designing, assembling, deploying, and recovering the tripods. Thanks to Captain Andy Reay-Ellers, the captain of the R/V Jack Robertson. Ongoing studies at the site have been motivated by the Snohomish Public Utility District and without their interest in tidal energy this study would not have been undertaken. Washington State Parks allowed for the placement of the AIS system on Admiralty Head Light-house and helped reboot the system after a number of power outages. We thank the anonymous reviewers for their comments on the content and structure of the manuscript. Funding provided by U.S. Department of Energy Award No. DE-EE0002654. Student support provided to C.B. by National Science Foundation Award No. DGE-0718124.

APPENDIX A: TRANSMISSION LOSSES COEFFICIENT

A single-valued transmission loss model [i.e., 15 log(r)] assumes that the transmission losses are independent of the location of a vessel relative to the hydrophone receiver. Given changing bathymetric profiles between the ship and receiver as a vessel travels in the shipping lanes, the assumption of angular and range independence must be verified. To justify the use of a single-valued transmission loss model, a

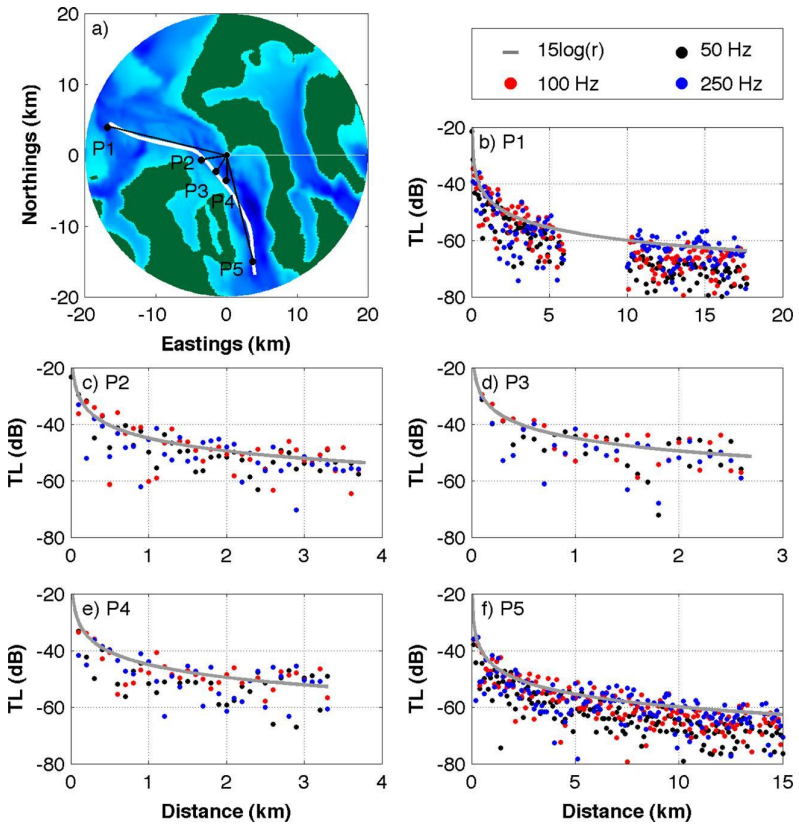

FIG. 9. (Color online) (a) Site map and profile locations used for the range dependent PE model. A typical ship track for southbound traffic is included (white line). (b)–(f). Transmission losses modeled at 50, 100, and 250 Hz and a comparison with the simplified model. For P1, the missing points are associated parts of the profile where the receiver depth of 57 m was below the water–sediment interface. The transmission loss is plotted every 100 m to reduce the clutter associated with the modal interference patterns. Each transmission loss plot ends at the location of the hydrophone deployment.

range dependent PE code (Collins, 2000) is used to calculate transmission losses for site-specific bathymetric profiles at three key frequencies. The modeled frequencies (50, 100, 250 Hz) covered the range of frequencies associated with peak spectrum levels of ship traffic at the site (Fig. 7).

Important inputs to the model include the geoacoustic parameters, bathymetry, water properties, and the source depth. No detailed information about the geophysical parameters throughout the site is available. However, studies in the immediate vicinity of the hydrophone deployments indicate that the bed is composed of a narrow layer (1–2 m thick) of gravel pavement above 40 m layer of sand interspersed with larger grains such as gravel (Landau Associates, 2011). For simplicity, the top pavement layer is neglected because it is small relative to the modeled wavelengths and additional deeper layers are neglected. The sediment properties for a coarse, gravely sand used in the model are a sound speed ratio of 1.25, a density ratio of 2.23, and an attenuation rate of 0.7 dB per wavelength (APL-UW, 1994). A constant sound speed of 1490 m s^{-1} is used in the water column because it is generally well-mixed (Polagye and Thomson, 2010). Available Puget Sound bathymetry data (Finlayson, 2005) are linearly interpolated to obtain the bathymetric profiles for modeled domains. The bathymetric profiles [P1–5, Fig. 10(a)] are typical of southbound traffic in the shipping lanes. Regardless of bearing, for ships traveling in the shipping lanes all bathymetric profiles are characterized by an upslope to shallower water at the hydrophone location near the headland. A source depth of 10 m was used to approximate the propeller depth of modern cargo vessels. A receiver depth of 57 m is used and is similar to the mean depth at which ambient noise measurements in the study were obtained.

The transmission loss curves for the modeled bathymetric profiles along with the simple transmission loss model are shown in Figs. 9(b)–9(f). In general, the single-valued transmission loss estimate predicts peak levels in the modal interference patterns to an acceptable degree. Shallow portions of profiles 1 and 5 (depth less than one acoustic wavelength) strip much of the energy from the 50 Hz modes and the simplified model performs poorly. However, the results are closer to the single-valued model at 100 and 250 Hz. The simplified model performs best near the CPA (P2-4). Noting that the simplified model, if anything, underestimates the total transmission losses, the overall agreement for the

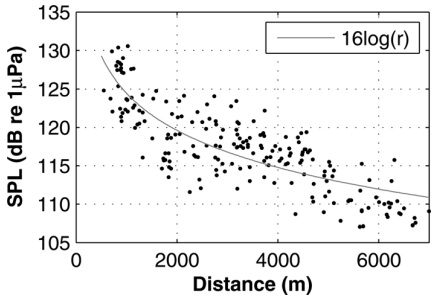

FIG. 10. Received levels (0.02–30 kHz) from local ferry traffic versus the distance between the ferry and the hydrophone.

typical variations in profiles justifies the use of the single-valued transmission loss model to reconstruct noise levels and estimate SL.

APPENDIX B: FERRY SL

To estimate the source level of the most commonly present vessel, the local ferry, and empirically estimate the transmission loss coefficient, acoustic data throughout the year were used. Current velocity and AIS data were used to screen for periods in which the currents were weak ($<0.4\,\mathrm{m\,s^{-1}}$) and the local ferry "Chetzemoka" was the only vessel in the study area. Further manual screening was done to remove recordings of the ferry that were not consistent with other ferry measurements and were deemed to be likely contaminated by other noise sources (e.g., a non-AIS equipped vessel). The source level and transmission loss coefficient were calculated by regressing the broadband RL against the log of the distance, in meters, and performing a least squares linear regression analysis. In this instance, estimation of the transmission loss coefficient for the ferry was limited by the Port Townsend ferry terminal at a distance of 7 km. The resulting regression fit yielded a source level of 173 dB re 1 μPa at 1 m (y intercept) and a transmission loss coefficient of 16 dB (slope). Figure 10 shows the results of the regression with the RL plotted against the distance to the ferry on a linear scale.

[1]For smaller vessels, including small U.S. flagged cargo vessels, tugs, fishing vessels, and vessels falling into the categories of "other" and "various," registration data (http://www.boatinfoworld.com/) were used. Searches by vessel name result in information that includes vessel type, size, and length, which were cross-checked against AIS data. Similarly, online fleet information was used for many commercial vessels to cross-check registration and AIS data (e.g., http://westerntowboat.com/Tugs/ to confirm registration data for the vessel Western Mariner; http://www.cosco.com/en/fleet/ to confirm COSCO fleet information).

Ainslie, M., and McColm, J. (**1998**). "A simplified formula for viscous and chemical absorption in sea water," J. Acoust. Soc. Am. **103**, 1671–1672.

Applied Physics Laboratory (**1994**). "High-frequency ocean environmental acoustic models handbook," Technical Report TR 9407, Applied Physics Laboratory at the University of Washington.

Arveson, P. T., and Vendittis, D. J. (**2000**). "Radiated noise characteristics of a modern cargo ship," J. Acoust. Soc. Am. **107**, 118–129.

Buckstaff, K. (**2004**). "Effects of watercraft noise on the acoustic behavior of bottlenoise dolphins, *Tursiops truncatus*, in Sarasota, Florida," Marine Mammal Sci. **20**, 709–725.

Clark, C., Ellison, W., Southall, B., Hatch, L., Van Parijs, S., Frankel, A., and Ponirakis, D. (**2009**). "Acoustic masking in marine ecosystems: Intuitions, analysis, and implications," Mar. Ecol.: Prog. Ser. **395**, 201–222.

Collins, M. D. (**2000**). "User's guide for RAM versions 1.0 and 1.0p," Naval Research Laboratory, Washington, DC.

Dahl, P., Miller, J., Cato, D., and Andrew, R. (**2007**). "Underwater ambient noise," Acoust. Today **3**, 23–33.

Ellison, W., Southall, B., Clark, C., and Frankel, A. (**2011**). "A new context-based approach to assessing mammal behavioral responses to anthropogenic sounds," Conserv. Biol. **26**, 1–8.

Erbe, C. (**2002**). "Underwater noise of whale-watching boats and potential effects on killer whales (*Orcinus orca*), based on acoustic impact model," Marine Mammal Sci. **18**, 394–418.

Federal Register (**2003**). "Automatic identification system; vessel carriage requirements," Coast Guard, U.S. Department of Homeland Security, pp. 60559–60570.

Finlayson D. P. (**2005**). "Combined bathymetry and topography of the Puget Lowland, Washington State," http://www.ocean.washington.edu/data/pugetsound/ (Last viewed July 16, 2012).

Foote, A., Osborne, R., and Hoelzel, A. (**2004**). "Whale-call response to masking boat noise," Nature (London) **428**, 910.

Frisk, G. V. (**2012**). "Noiseonomics: The relationship between ambient noise levels in the sea and global economic trends," Sci. Rep. **107**, 1–4.

Gray, L., and Greeley, D. (**1980**). "Source level model for propeller blade rate radiation for the world's merchant fleet," J. Acoust. Soc. Am. **67**, 516–522.

Greene, C. R., Jr., and Moore, S. (**1995**). "Man-made noise," in *Marine Mammals and Noise*, edited by J. W. Richardson, C. R. Greene, Jr., C. I. Malme, and D. H. Thompson (Academic, San Diego), pp. 101–158.

Harati-Mokhtari, A., Wall, A., Brooks, P., and Wang, J. (**2007**). "Automatic identification system (AIS): Data reliability and human error implications," J. Navig. **60**, 373–389.

Hatch, L., Clark, C., Merrick, R., Van Parijs, S., Ponirakis, D., Schwehr, K., Thompson, M., and Wiley, D. (**2008**). "Characterizing the relative contributions of large vessels to total ocean noise fields: A case study using the Gerry E. Studds Stellwagen Bank National Marine Sanctuary," Environ. Manage. (N.Y.) **42**, 735–752.

Hildebrand, J. (**2004**). "Sources of anthropogenic sound in the marine environment," Technical Report, Report to the Policy on Sound and Marine Mammals: An International Workshop, U.S. Marine Mammals Commission and Joint Conservation Committee U.K., London.

Hildebrand, J. (**2005**). "Impacts of anthropogenic sound," in *Marine Mammal Research: Conservation Beyond Crisis*, edited by J. E. Reynolds, W. F. Perin, R. R. Reeves, S. Montgomery, and T. J. Ragen (The Johns Hopkins University Press, Baltimore, MD), pp. 101–124.

Hildebrand, J. (**2009**). "Anthropogenic and natural sources of ambient noise in the ocean," Mar. Ecol.: Prog. Ser. **395**, 5–20.

Holt, M., Noren, D., Veirs, V., Emmons, C., and Veirs, S. (**2009**). "Speaking up: Killer whales (*Orcinus orca*) increase their call amplitude in response to vessel noise," J. Acoust. Soc. Am. **125**, EL27–EL32.

Kipple, B. (**2004a**). "Coral Princess underwater acoustic levels," Technical Report (Naval SurfaceWarfare Center, Bremerton Detachment).

Kipple, B. (**2004b**). "Volendam underwater acoustic levels," Technical Report (Naval Surface Warfare Center, Bremerton Detachment).

Kipple, B., and Gabriele, C. (**2003**). "Glacier Bay watercraft noise: Report to Glacier Bay National Park by the Naval Surface Warfare Cent-Detachment Bremerton," Technical Report No. NSWCCD-71-TR-2003/522.

Landau Associates (**2011**). "Preliminary geologic characterization: Proposed tidal turbine site Island County, Washington," Technical Report for Sound and Sea Technology and Snohomish County, P. U. D., September 6, 2011.

Lee, S., Kim, S., Lee, Y., Yoon, J., and Lee, P. (**2011**). "Experiment on effect of screening hydrophone for reduction of flow-induced ambient noise in ocean," Jpn. J. Appl. Phys. **50**, 1–2.

McDonald, M. A., Hildebrand, J. A., and Wiggins, S. M. (**2006**). "Increases in deep ocean ambient noise in the Northeast Pacific west of San Nicolas Island, California," J. Acoust. Soc. Am. **120**, 711–718.

McDonald, M. A., Hildebrand, J. A., Wiggins, S. M., and Ross, D. (**2008**). "A 50 year comparison of ambient ocean noise near San Clemente Island: A bathymetrically complex coastal region off Southern California," J. Acoust. Soc. Am. **124**, 1985–1992.

McKenna, M., Ross, D., Wiggins, S., and Hildebrand, J. (**2012**). "Underwater radiated noise from modern commercial ships," J. Acoust. Soc. Am. **131**, 92–103.

National Marine Fisheries Service (NMFS) (**2005**). "Endangered fish and wildlife; notice of intent to prepare an environmental impact statement," Federal Register **70**(7), 1871–1875 (Docket No. 05-525, 11 January 2005).

National Marine Fisheries Service (NMFS) (**2006**). "Endangered and threatened species; designation of critical habitat for Southern Resident killer whales," Federal Register **71**(229), 69054–69070 (Docket No. 060228057-6283-02, 29 November 2006).

National Research Council of the U.S. National Academies (NRC) (**2000**). *Marine Mammals and Low-Frequency Sound* (National Academy Press, Washington, DC), pp. 7, 76.

National Research Council of the U.S. National Academies (NRC) (**2003**). *Ocean Noise and Marine Mammals* (National Academy Press, Washington, DC), pp. 6, 65–67, 89, 93, 128.

National Research Council of the U.S. National Academies (NRC) (**2005**). *Marine Mammal Populations and Ocean Noise: Determining When Ocean Noise Causes Biologically Significant Effects* (National Academy Press, Washington, DC), p. 14.

Orlanski, I. (**1975**). "A rational subdivision of scales for atmospheric processes," Bull. Am. Meteorol. Soc. **56**, 527–530.
Polagye, B., and Thomson, J. (**2010**). "Admiralty Inlet water quality survey report: April 2009–February 2010," Technical Report, Northwest National Marine Renewable Energy Center, University of Washington, Seattle, WA.
Rolland, R. M., Parks, S. E., Hunt, K. E., Castellote, M., Corkeron, P. J., Nowacek, D. P., Wasser, S. K., and Kraus, S. D. (**2012**). "Evidence that ship noise increases stress in right whales," Proc. R. Soc. London, Ser. B **279**, 2363–2368.
Ross, D. (**1976**). *Mechanics of Underwater Noise* (Permagon, Elmsford, NY), pp. 272, 279–280.
Schwehr, K. (**2010**). "Python software for processing AIS data. v0.43," http://vislab-ccom.unh.edu/schwehr/software/noaadata (Last viewed January 29, 2011).
Scrimger, P., and Heitmeyer, R. (**1991**). "Acoustic source-level measurements for a variety of merchant ships," J. Acoust. Soc. Am. **89**, 691–699.
Southall, B. (**2005**). "Shipping noise and marine mammals: A forum for science, management, and technology," Technical Report, Final Report of the National Oceanic and Atmospheric Administration (NOAA) International Symposium, U.S. NOAA Fisheries, Arlington, VA, May 18–19, 2004.
Southall, B., Bowles, A., Ellison, W., Finneran, J., Gentry, R., Greene, C., Jr., Kastak, D., Ketten, D., Miller, J., Nachtigall, P., Richardson, W., Thomas, J., and Tyack, P. (**2007**). "Marine mammal noise exposure criteria: Initial scientific recommendations," Aquat. Mamm. **33**, 411–521.
Thomson, J., Polagye, B., Durgesh, B., and Richmond, M. C. (**2012**). "Measurements of turbulence at two tidal energy sites in Puget Sound, WA," IEEE J. Ocean. Eng. **37**, 363–374.
Thorne, P. (**1990**). "Seabed generation of ambient noise," J. Acoust. Soc. Am. **87**, 149–153.
Thorne, P. D., Heathershaw, A. D., and Troiano, L. (**1984**). "Acoustic detection of seabed gravel movement in turbulent tidal currents," Mar. Geol. **54**, M43–M48.
Trevorrow, M. V., Vasiliev, B., and Vagle, S. (**2008**). "Directionality and maneuvering effects on a surface ship underwater acoustic signature," J. Acoust. Soc. Am. **107**, 767–778.
Urick, R. (**1967**). *Principles of Underwater Sound for Engineers* (McGraw-Hill, New York), pp. 164–165.
Van Parijs, S., Clark, C., Sousa-Lima, R., Parks, S., Rankin, S., Risch, D., and Van Opzeeland, I. (**2009**). "Management and research applications of real-time and archival passive acoustics sensors over varying temporal and spatial scales," Mar. Ecol.: Prog. Ser. **395**, 21–36.
Veirs, S., and Veirs, V. (**2005**). "Average levels and power spectra of ambient sound in the habitat of southern resident orcas," NMFS Contract Report No. AB133F05SE6681.
Wenz, G. (**1962**). "Acoustic ambient noise in the ocean: Spectra and sources," J. Acoust. Soc. Am. **34**, 1936–1956.